

Research Article

Design of Compact Open-Ended Wrench-Shaped Patch Antenna for 5G Sub-6 GHz Band Applications

Mahadi Hassan, Abu Zafor Muhammad Touhidul Islam * 

Department of Electrical & Electronic Engineering, University of Rajshahi, Rajshahi, Bangladesh
E-mail: touhid.eee@ru.ac.bd

Received: 27 December 2024; **Revised:** 31 January 2025; **Accepted:** 10 February 2025

Abstract: The 5G network requires higher frequency bands as the Sub-6 GHz to handle vast amounts of data and to provide larger bandwidth. This study proposes a novel open-ended wrench-shaped patch antenna with small dimensions of $24 \times 32 \times 1.6 \text{ mm}^3$ to achieve wideband operation in the Sub-6 GHz range. The antenna is etched onto an FR-4 substrate and has dimensions of 1.6 mm in height, a loss tangent of 0.025, and a relative permittivity of 4.3. The intended antenna is excited by a 50Ω microstrip line, and the simulation is performed using CST software. The impedance matching and antenna bandwidth are improved by introducing a slotted patch plane with a defective ground structure. With two resonance frequencies of 3 GHz and 4.55 GHz, the suggested antenna has a gain of 1.91 dB to 2.90 dB, a directivity of 2.62 dB to 4.13 dB, a return loss of -58.5 dB and -28.4 dB , and a VSWR of 1.002 and 1.08. The wrench's open-ended design provides a broad 3.2 GHz impedance bandwidth and a maximum radiation efficiency of 85.7% in the frequency range of 2.6 to 5.8 GHz, encompassing multiple crucial bands utilized for various applications, including 5G. The design offers significant size reduction while maintaining excellent performance characteristics suitable for 5G wireless devices operating frequency of Sub-6 GHz. The suggested antenna has been built as an experimental prototype, and the results of the measurement and modeling of the return loss parameter coincide quite well.

Keywords: wrench-shaped patch antenna, 5G, Sub-6 GHz, wideband, slotted partial ground plane

1. Introduction

Fifth-generation (5G) networks are now positioned as a key component of future connectivity because of their quick enhancement of wireless communication systems and rises in data consumption. 5G promises enhanced data rates, reduced latency, and increased network capacity, catering to a broad range of uses spanning from Internet of Things (IoT) devices to high-definition multimedia streaming.

Microstrip patch antennas have become highly versatile and adaptable for sub-6 GHz frequencies through the application of these techniques. While challenges like limited bandwidth, efficiency, and size persist, advanced design strategies such as material optimization, geometry modifications, and array configurations help overcome these obstacles and the growing necessity of modern wireless systems. To understand the full capability of 5G, it is imperative to develop an efficient and compact antenna that is capable of operating within a frequency band of Sub-6 GHz.

In reference [1], a compact and highly efficient patch antenna has been designed on Rogers RT 5880 substrate for WiMAX and lower 5G communications. The mentioned microstrip antenna dedicates excellent bandwidth with efficiency

while fostering a compact size. In [2], increasing the substrate thickness raises the antenna performance by up to 20%. In [3], the authors focused on designing and optimizing an inset-fed rectangular microstrip patch antenna by adjusting the inset gap and inset length to enhance gain and efficiency. A parametric analysis of the surface current distribution and reflection coefficient is performed in [4] to examine the strip and slot's behavior at resonance ranges of frequencies. Financial technology is examined in [5] to promote high-quality economic development, reduce financial sector risks, and stimulate business innovation. In [6], a simple microstrip patch antenna and a 4-element array are employed for 5G wireless communication, achieving high gain, bandwidth, radiation efficiency, and directivity. The pi-shaped slotted patch antenna in [7] demonstrates omni-directional characteristics across the entire band of frequency, a critical spectrum range allocated for 5G deployment [8, 9].

Numerous design efforts on the design of microstrip antennas have been undertaken to confirm reliable characteristics in the 5G communication bands [10, 11]. Some notable achievements and challenges are outlined below: A novel compact antenna design has been created, featuring a semi-circular structure and an arc-shaped opening in its radio frequency front section, enabling it to function across two frequency bands. The arc-like slot interconnects the main semi-circular cuts, allowing antenna to resonate at frequencies near 1.8 GHz and 2.4 GHz, while providing strong peak gain. The antenna, referenced in [12], has dimensions of $30 \times 28.5 \times 0.8 \text{ mm}^3$, making it ideal for use in digital communication systems. Furthermore, a patch antenna of Y-shaped, with size of $55 \times 34 \times 1 \text{ mm}^3$ and a partial ground plane, has been suggested in [13] for medical applications and low-frequency 5G usage, demonstrating improved antenna gain compared to a full ground plane. A single-fed multiband Franklin strip antennas designed for 4G and 5G communication systems, with dimensions of $45 \times 40 \times 0.508 \text{ mm}^3$, was mentioned in [14], utilizing both HFSS and CST tools for simulations. A distinct antenna with a square-shaped patch design featuring slots in the shape of a diamond were investigated as referenced in [15], achieving a frequency range of 1.04 GHz. Furthermore, as referenced in [16], a printed dipole antenna operating on two frequency bands was designed for 5G networks developed and manufactured. Additionally, a compact portable patch with a semi-circular shape antenna was created for frequencies below 6 GHz range in 5G was demonstrated 80% efficiency and with a 5 dB gain, with antenna characteristics enhanced utilizing a partial ground-plane method. Research in an LTCC antenna module designed for 5G incorporated a patch design along with a strapline-fed network to achieve wide bandwidth.

An increase in bandwidth was suggested through the use of patch antennas with parasitic elements, which also produced a consistent radiation pattern [17]. Employing coplanar parasitic components in place of adding a passive patch antenna placed on top decreased the layer count but complicated the tuning process [18]. A pair of antennas designed for 5G wireless communication in drone applications were suggested, utilizing Rogers RT 5880 (lossy) material for its lower dielectric constant, allowing attachment to any flat UAV surface. Despite its high efficiency, this antenna's bandwidth was limited to approximately 0.702 GHz [19]. For wireless sensor application systems, an ultra-wideband antenna based on Rogers RT 5880 with quadruple rejection bands was proposed. By including four R-CSRRs into the patch and positioning two RSSRRs close to the feed of a traditional radiator, quintuple rejection frequency bands were accomplished [20]. Additionally, 4 complementary split-ring resonators (CSRRs) were employed in [21], leading to create a radiator with dimensions of $40 \times 30 \times 0.81 \text{ mm}^3$. A 5G broad-spectrum patch antenna with a rectangular slot at the top of the ground plane to reach the chosen operating band was described in [22]. The antenna's peak efficiency was 87.13%, its highest gain was 4.21 dBi, and its average gain was 0.34 dBi. System efficiency was shown to enhance when Rogers RT 5880 (lossy) material was added to a 5G radiator [23]. 5G communication in the Sub-6 GHz region was addressed using an inset feed approach [24]. Also, a circular monopole antenna with a patch design employing a spanner-shaped feed method was proposed [25]. Also, a kite-shaped planar antenna was studied, taking into account the impact of the ground plane, changes in a rectangular gap in the ground plane, and adjustments to the emitting patch's dimensions [26]. Furthermore, [27] described in detail the design and analysis of a wrench-shaped microstrip-fed square-shaped patch radiator with a changed ground plane and a stepped slot for various wireless communication applications.

In this study, a novel patch antenna with a unique open-ended wrench-like shape that is optimized for sub-6 GHz operation is designed and its performance is analyzed. Built on a small FR-4 substrate, the antenna has a slotted partial ground plane. The open-ended spanner-shaped patch antenna exhibits improved performance in gain, directivity, and efficiency over a frequency between 2.6 GHz to 5.8 GHz, providing a total bandwidth of 3.2 GHz. The lossy FR-4 had been used as the substrate material for the proposed antennas despite being lossy for the following reason: FR-4 is

relatively inexpensive compared to other materials, is easily accessible and is manufactured in large quantities, it offers good mechanical stability, ease of fabrication and acceptable performance.

The structure and design details for the suggested antenna are explored in Section 2, Simulation results with discussion, and a comparison analysis is provided in Section 3, and the conclusion is added in Section 4.

2. Structural design of suggested antenna

On a low-loss FR-4 (lossy) substrate, a tiny, open-ended wrench-shaped circular microstrip patch antenna is designed and simulated with a ϵ_r of 4.3 and a $\tan(\delta)$ of 0.025. The substrate has a height of 1.6 mm and is used in the structured antenna designs, with simulations performed using CST Studio Suite 2018 software. The antenna was initially structured with a resonance frequency of 3 GHz. The radiating patch and slotted partial ground plane are made of annealed copper, which is 0.035 mm thick. The wrench-shaped patch antenna in question has final measurements of $24 \times 32 \times 1.6 \text{ mm}^3$. A microstrip feed line is applied to supply microwave power to this antenna. The suggested antenna structure's front, rear, side, and enlarged views are shown in Figure 1.

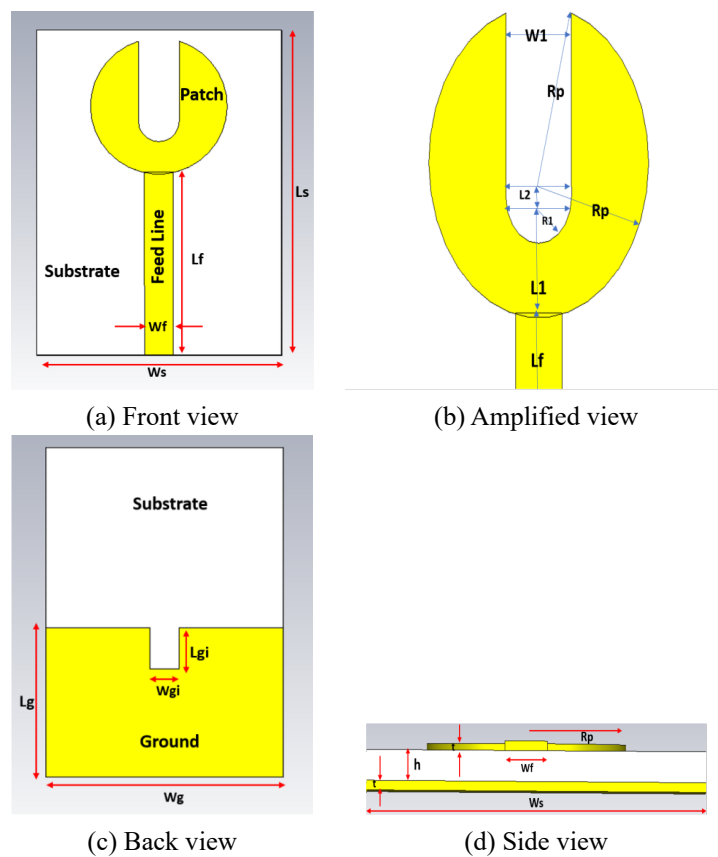


Figure 1. Geometrical structure of the structured antenna

For antenna design, it is assumed that the ϵ_r , f_r in GHz, and h in mm are provided. Using these parameters, a set of simplified cavity model equations can be applied for calculating the design parameters for the microstrip patch antenna. The patch's radius (R) is established by [28]:

$$a = \frac{F}{\left[1 + \frac{2h}{\pi F \epsilon_r} (\ln\{\pi F / 2h\} + 1.7726)\right]^{0.5}} \quad (1)$$

where, a denotes the patch radius, h represents the dielectric substrate's thickness, ϵ_r is the substrate relative dielectric constant and F is the logarithmic function.

$$F = \frac{8.791 \times 10^9}{f_r \sqrt{\epsilon_r}} \quad (2)$$

where f_r is resonance frequency

The substrate's length and width can be found by,

$$\text{Substrate length, } L_s = 2 \times 2a \quad (3)$$

$$\text{Substrate width, } W_s = 2 \times 2a \quad (4)$$

CST software is used to model a small, open-ended patch antenna in wrench shape. The design process of the mentioned antenna unfolds in several steps. Initially, it is assumed that ϵ_r, f_r in GHz, and h in mm are known. Using this information, a set of simplified cavity model Equations (1)–(4) is employed for calculating the geometrical properties of the antenna. The performance required for the intended applications is then attained by using and modifying a variety of strategies, including the use of slots and partial ground planes. To target 5G applications, the design starts with an antenna model (step 1) that is optimized for its geometric dimensions and lacks slots. Subsequently, slots are progressively introduced on the patch to create a wrench-shaped open-ended structure. The radiation performance is carefully monitored and the dimensions (width and radius) of the slots are fine-tuned after each step, based on the observed radiation response. The dimensions of these patch slots and values of other design parameters for the suggested miniature patch antenna are presented in Table 1.

The feeder line, with dimensions of $2.83 \times 18 \text{ mm}^2$ is powered and delivered to the wrench-shaped emitting patch, which has a diameter of 6.7 mm. A rectangular slot (defected ground structure) with optimal dimensions of 3 mm in width and 4 mm in length is incorporated into the partial ground plane rising the impedance matching and bandwidth of the antenna. The slot's location has been adjusted to provide the best performance for sub-6 GHz applications.

Table 1. Parameters of the optimized design of the structured antenna

Parameters with their symbol	Value (mm)
Substrate's Width, W_s	24
Substrate's Length, L_s	32
Feeder's Width, W_f	2.83
Length of Feeder, L_f	18
Ground's Width, W_g	24
Ground's Length, L_g	14.5
Radius of patch, R_p	6.7
Slot width of ground, W_{gi}	3
Slot length of ground, L_{gi}	4
Patch slot width, W_1	4
Radius of patch slot, R_1	2
L1	5
L2	1.5
Thickness of Patch & Ground, t	0.035
Substrate's thickness, h	1.6

3. Results and discussion

The simulations for different parameters of the mentioned open-ended wrench-shaped microstrip patch antenna are provided and examined in the below sections.

3.1 Loss of return

Figure 2a illustrates the changes in return loss with operational antenna frequency. The antenna's lower and upper ends have -10 dB frequencies of 2.6 GHz and 5.8 GHz, respectively, while its two core frequencies are at 3 GHz and 4.55 GHz. The Sub-6 GHz band includes this frequency range. At 3 GHz, this antenna exhibits an impressive S11-parameter value of -58.7 dB, indicating strong return loss and efficient impedance matching. This suggests highly effective signal transmission and reception within the desired frequency band. At 4.55 GHz, although the S11-parameter value is slightly higher at -28.5 dB, it still signifies good performance in return loss and acceptable impedance matching, ensuring reasonable transmission efficiency.

3.2 Bandwidth

It is seen from Figure 2a that the designed antenna performs at two center frequencies, $f_{c1} = 3$ GHz and $f_{c2} = 4.55$ GHz, with -10 dB lower $f_{CL} = 2.6$ GHz and higher cut-off frequency, $f_{CH} = 5.8$ GHz within the Sub-6GHz frequency band. Hence the operating -10 dB bandwidth of this antenna is $BW = 3.2$ GHz which covers the most popular 5G range (3.33–4.2 GHz), WiMax rel 2 (3.4–3.6 GHz), Wifi-5 (5.15–5.85 GHz) band applications.

3.3 VSWR

Figure 2b displays the voltage standing wave ratio (VSWR) versus frequency plot for the designed patch antenna. The VSWR values at the two frequencies of 3 GHz and 4.55 GHz, are 1.002 and 1.08, respectively. At 3 GHz, the antenna exhibits an exceptionally low VSWR of 1.002, indicating excellent impedance matching and minimal power loss due to reflection. This suggests highly effective signal transmission and reception at this frequency, resulting in well-suited for 5G applications requiring reliable communication within the Sub-6 GHz. At 4.55 GHz, the antenna maintains a slightly higher VSWR of 1.08, which still reflects good impedance matching and reasonable transmission efficiency. These VSWR values remain within acceptable limits.

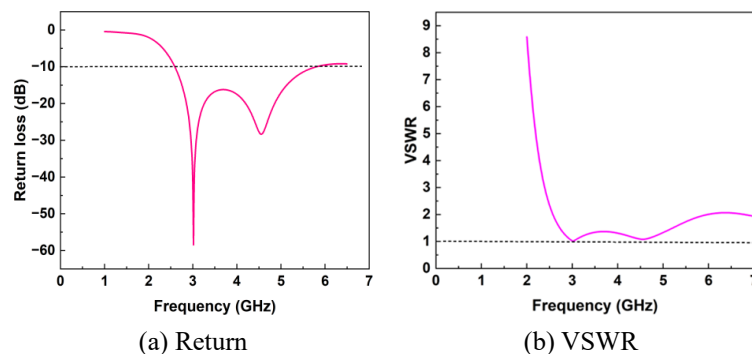


Figure 2. (a) Loss of return vs frequency and (b) VSWR vs. frequency of the mentioned antenna

3.4 Gain

The plot of the antenna gain fluctuations with frequency for the suggested antenna is displayed in Figure 3a. The gain refers to the measure of how effectively an antenna can focus energy in a fixed direction than an ideal isotropic radiator. It quantifies the capability of the antenna to direct its radiated energy toward a fixed direction, typically expressed in dB

(decibels). At 3 GHz, the antenna gain is 1.91 dB, indicating moderate directional amplification of signals at this frequency. The indicated antenna performs a maximum gain of 2.90 dB at 5.2 GHz, reflecting improved amplification of signals at this frequency. These gain value suggests effective transmission and reception of signal within the desired frequency band, and hence the antenna contributing to reliable communication performance in 5G applications. Figure 4 at $\phi = 90$ degrees displays the polar plot of the far-field gain of the planned antenna at the resonance frequencies of 3 GHz and 4.5 GHz. The obtained main lobe magnitudes are 2.15 dB V/m at 3 GHz and 2.75 dB V/m at 4.5 GHz. The lobe directions are 166° and 148° , the 3 dB angular beam-width (or half power beam-widths) are 93.9 and 90.7° , and the side lobe levels are -1.9 dB and -4.4 dB these resonant frequencies.

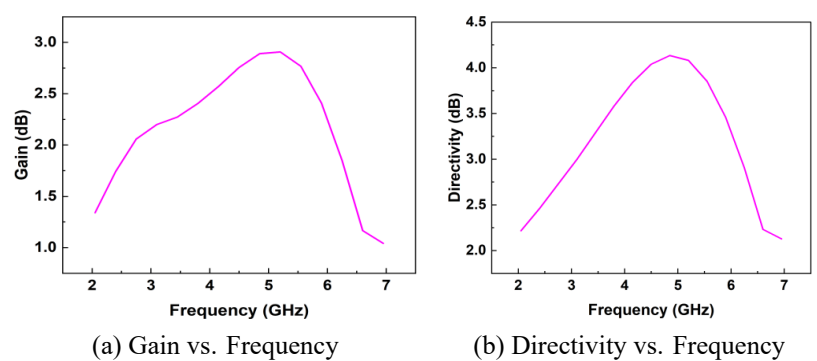


Figure 3. Frequency dependent (a) Gain and (b) Directivity plots

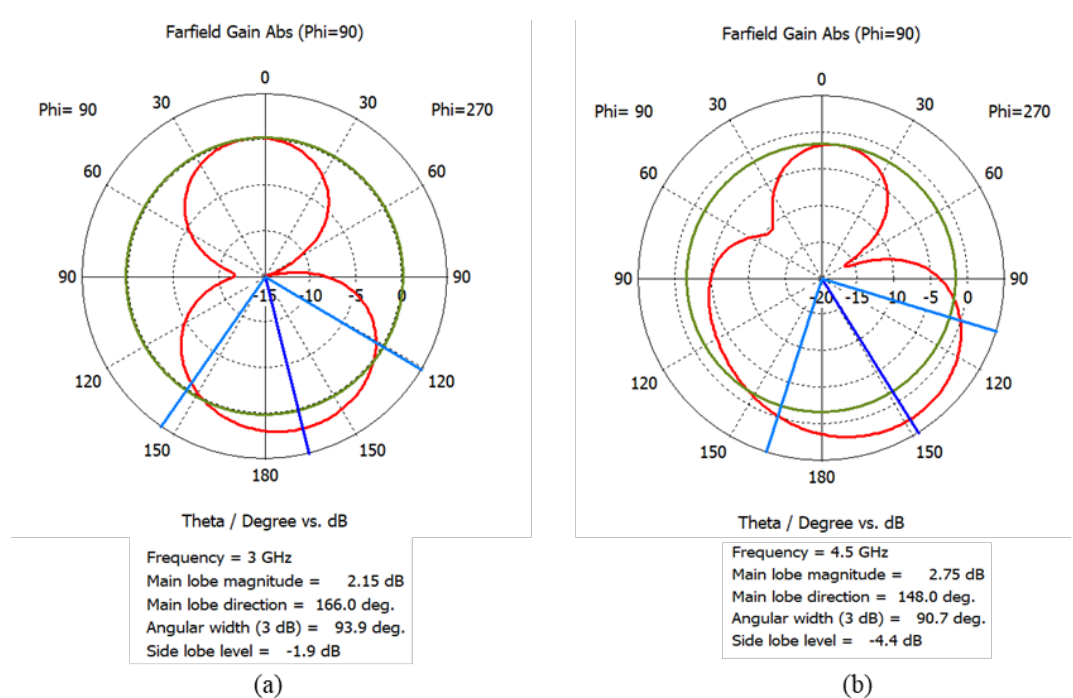


Figure 4. Polar plot of the farfield gain at 3 GHz and 4.5 GHz ($\phi = 90$ degree) of the designed antenna

The plot of variations of antenna gain with frequency of the designed antenna is depicted in Figure 3a. At 3 GHz, the antenna demonstrates a gain of 1.91 dB, indicating moderate directional amplification of signals at this frequency. The mentioned antenna performs a maximum gain of 2.90 dB at 5.2 GHz, reflecting improved amplification of signals at this frequency.

While the gain of (1.91–2.90) dB is lower than other 5G antenna designs, this trade-off is offset by the antenna size and bandwidth of 3.2 GHz. These attributes ensure compatibility with applications requiring a small form factor and support high data rates, particularly for short-range or indoor environments such as IoT networks and small-cell deployments. While the gain of (1.91–2.90) is relatively low, it is acceptable for applications where short-range communication and compact size are essential, such as IoT and small-cell deployments. These scenarios benefit more from wide bandwidth and compact designs than from high gain.

The indicated antenna's far field gain patterns at 3 GHz and 4.5 GHz are shown in Figure 4. The study does not explicitly address or show cross-polarization components there, which are critical for assessing polarization purity and overall performance. The obtained main lobe magnitudes are 2.15 dB V/m at 3 GHz and 2.75 dB V/m at 4.5 GHz. The lobe directions are 166° and 148°, the 3 dB angular beam-width (or half power beam-widths) are 93.9 and 90.7°, and the side lobe levels are -1.9 dB and -4.4 dB of these resonant frequencies. The observed radiation patterns indicate low side lobe levels, ensuring focused energy delivery in the desired direction with minimal energy leakage in undesired directions. The cross-polarization levels are minimal, achieving cross-polarization discrimination values exceeding 12 dB, which indicates the co-polarized component is much stronger than the cross-polarized one, implying good polarization purity and it aligns with the requirements for polarization-specific applications in 5G networks.

3.5 Directivity

The directivity of a patch antenna indicates its capacity to direct electromagnetic radiation towards a specific direction. Figure 3b illustrates the changes of directivity with frequency for the structured antenna. As seen, the directivity is as 2.62 dBi at lower-cutoff frequency 2.6 GHz and 4.13 dBi at upper-cutoff frequency 5.8 GHz. At 3 GHz, the antenna directivity is 2.92 dBi which demonstrates a relatively efficient concentration of radiation in a specific direction, resulting in increased signal strength and coverage in that direction compared to other directions. The directivity of 4.04 dBi at 4.55 GHz indicates that the antenna is even more efficient at focusing its radiation in a specific direction at that frequency compared to 2.6 GHz. The maximum directivity of 4.13 dBi of the structured antenna is obtained at 5.8 GHz. The 3D far-field directivity pattern of the designed antenna at the resonance frequencies of 3 GHz and 4.55 GHz is represented in Figure 5, with the observation taken at $\phi = 90$ degrees.

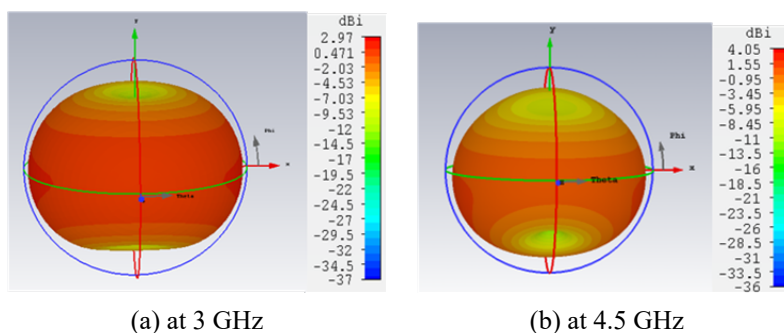


Figure 5. 3D farfield directivity pattern of the mentioned antenna

3.6 Radiation efficiency

Figure 6 shows the structured antenna's radiation efficiency versus frequency. Radiation efficiency measures how effectively a patch antenna transforms electrical energy into emitted electromagnetic energy. The radiation efficiency varies from 74.5% to 85.7% within the bandwidth indicates the antenna's efficiency in transforming electrical energy into radiated electromagnetic energy across different frequencies or within its operational bandwidth. When the radiation efficiency is 74.5%, it means that approximately 74.5% of input power supplied to the antenna was effectively radiated as electromagnetic waves, while the remaining percentage may be lost as heat or reflected power. Similarly, when the

radiation efficiency increases to 85.7%, a higher percentage of input power is transformed into emitted electromagnetic energy, resulting in improved radiator performance. At 2.6 GHz, the antenna gains a highest efficiency of 85.7%.

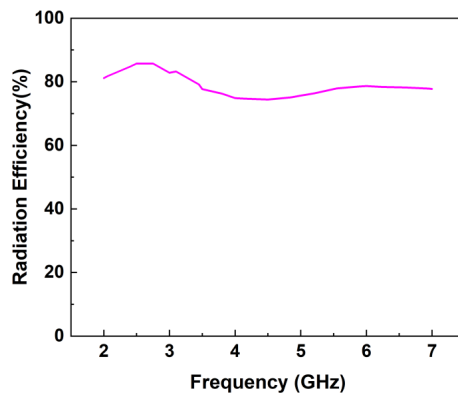


Figure 6. Frequency dependent radiation efficiency

3.7 Radiation pattern

Figures 7 and 8 display the polar plots of the far-field E-field pattern for the planned antenna at 3 GHz and 4.55 GHz, respectively, for $\phi = 0$ and $\phi = 90$ degrees. The antenna's 3D radiation patterns at the resonant frequencies of 3.55 GHz and 4.55 GHz, respectively, are shown in Figure 9a. The designed antenna focuses on its directional radiation pattern at two center frequencies within the Sub-6GHz frequency band. As seen, at 3 GHz the antenna performs a well-defined radiation pattern around the axis of the antenna. This feature is crucial for providing consistent range in a 360-degree field of view, essential for applications requiring seamless connectivity, such as IoT devices and mobile communications.

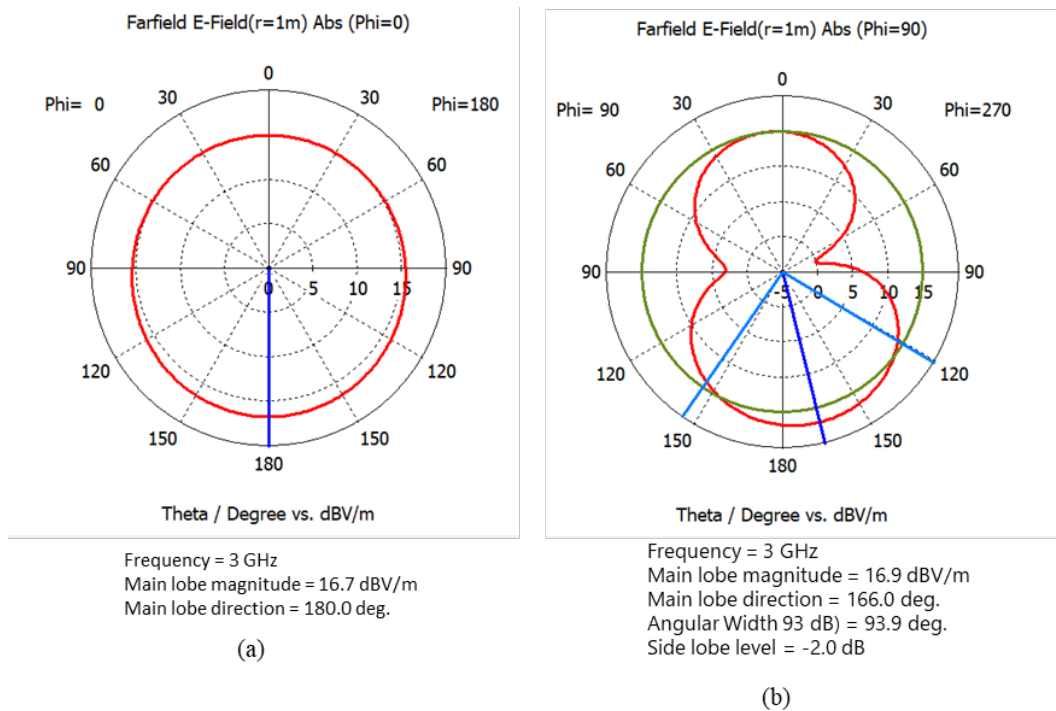


Figure 7. Farfield E-field ($\phi = 0$ and 90 degrees) of the structured antenna at 3 GHz

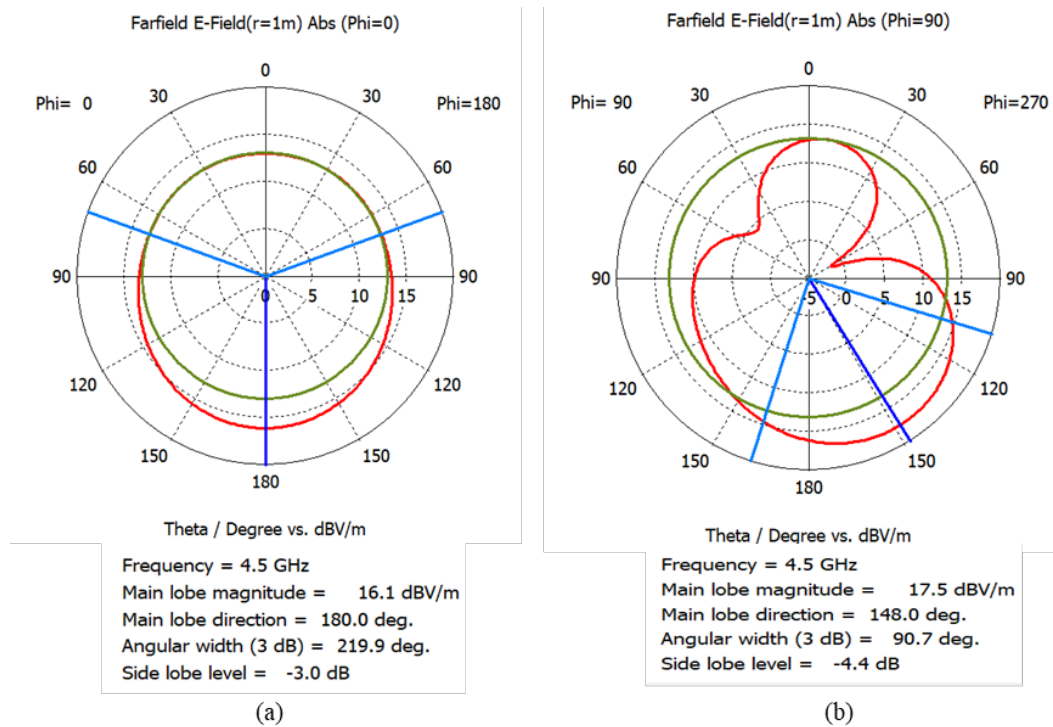


Figure 8. Farfield E-field ($\phi = 0$ and 90 degrees) of the designed antenna at 4.5 GHz

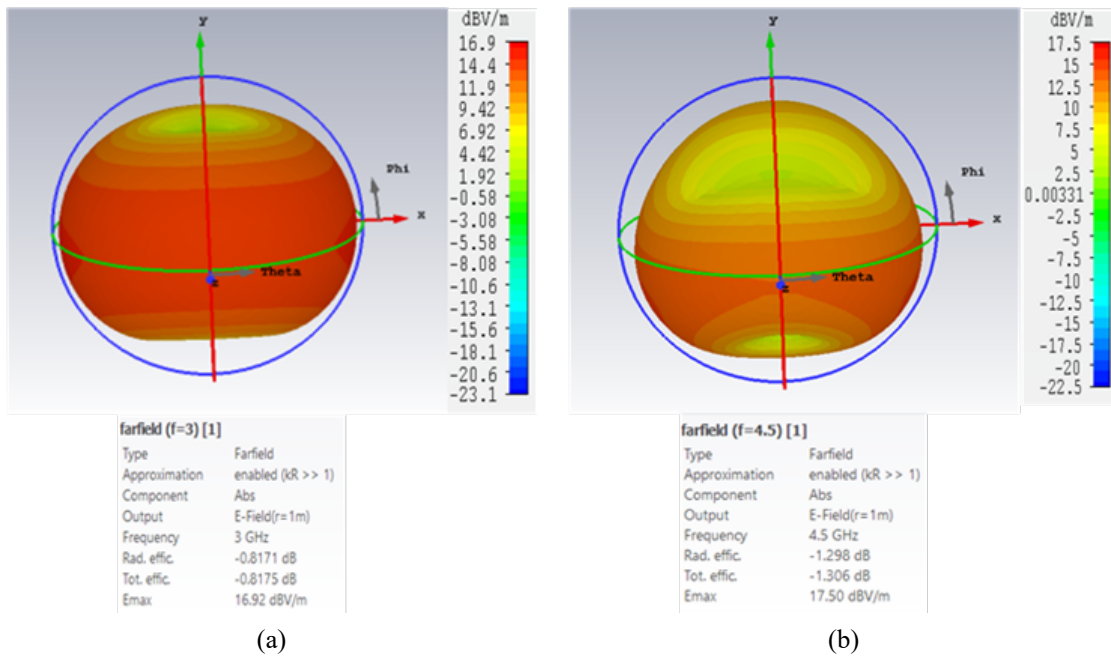


Figure 9. 3D farfield E-Field radiation pattern at (a) 3 GHz (b) 4.5 GHz

3.8 Surface current distribution

The structured antenna demonstrates excellent distribution of current across its radiating patch, with the current density reaching a peak of 59.98 A/m at 3 GHz and 52.57 A/m at 4.55 GHz, as illustrated in Figure 10. As seen, maximum

current is distributed along the at the feeder and patch edge of the antenna. This dispersion is attributed to the innovative design of the open-ended wrench-curved radiator and the selected partially slotted ground plane which collectively enable resonance at 3 GHz. The partially slotted ground plane improves coupling effects, leading to an expanded frequency range for the antenna across the 5G frequency band.

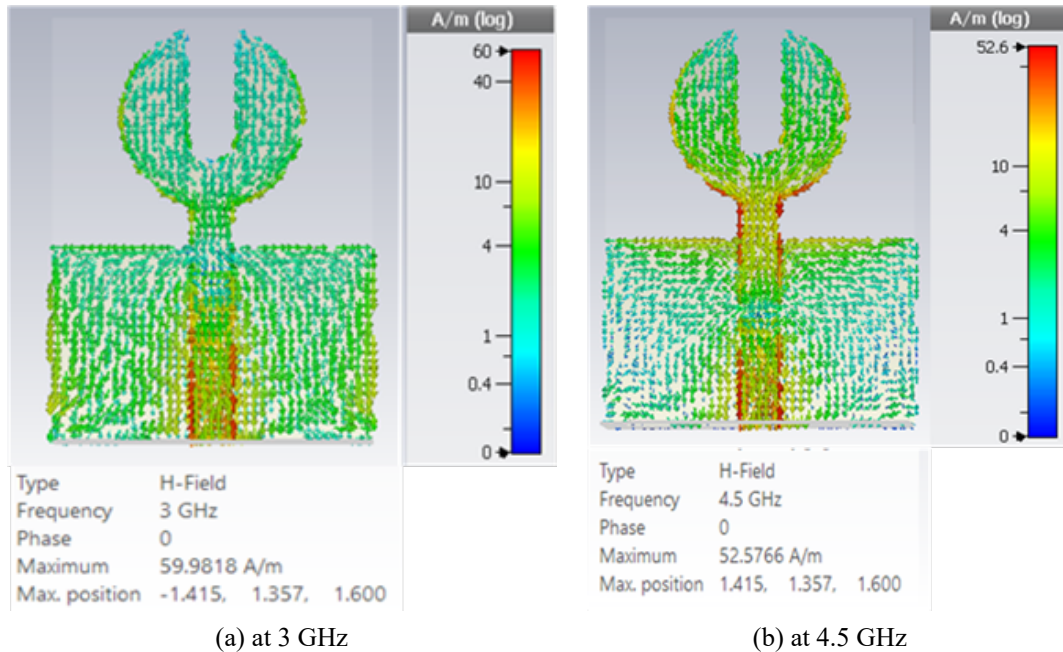


Figure 10. Distribution of surface current of the structured antenna

3.9 Comparison between proposed antenna and existing researches

The performance parameters of the structured antenna and those of antennas that were previously built and discovered in the literature review are contrasted in Table 2. The suggested antenna is somewhat smaller than the other antennas on the list, measuring $32 \times 24 \times 1.6 \text{ mm}^3$. The antenna boasts a broad operating frequency range of 2.6 GHz to 5.8 GHz, a high bandwidth of 3.2 GHz, and exceptional return losses of -58 dB and -28.4 dB at the two center frequencies of 3.55 GHz and 4.55 GHz, respectively. Though the proposed antenna has less gain compared to other designed antennae, it exhibits higher directivity of 2.62 to 4.13 dB and good radiation efficiency of 74.5 to 85.7% within the frequency range.

A low-profile, small, wrench-shaped, open-ended microstrip patch antenna with a slotted partial ground plane (defected ground structure, or DGS) is presented in this paper for 5G applications. The wrench shape is introduced in this patch antenna design for the first time. The wrench-shaped antenna provides an impressive wide bandwidth of 3.2 GHz and a reflection coefficient ($|S_{11}|$) of -58.5 dB . The antenna's 3.2 GHz bandwidth makes it ideal for 5G applications since it can function effectively across a broad frequency range. 5G technology covers several frequency bands, including sub-6 GHz. A wide impedance bandwidth ensures that the antenna can handle the various bands used by 5G networks, providing greater flexibility and better performance in different operating conditions. So, an antenna with a 3.2 GHz bandwidth would be well-suited for many of the frequency ranges utilized in 5G communications. A reflection coefficient ($|S_{11}|$) of -58.5 dB indicates excellent impedance matching. A reflection coefficient that is closer to $-\infty \text{ dB}$ means that less power is reflected, which means that more power is delivered from the source to the load with fewer reflections. A value of -58.5 dB suggests that almost all the power is being transferred with very little reflection, indicating efficient impedance matching.

The frequency range of 2.6 GHz to 5.8 GHz covers several essential bands used for diverse applications, including 5G. The frequency bands around this range play a critical role in various wireless communication systems. Here are a few significant applications: 4G LTE Bands, Wi-Fi, 5G Sub-6 GHz Bands, Fixed Wireless Access (FWA), Industrial, Scientific, and Medical (ISM) Bands applications. These frequencies provide both coverage and capacity, making them essential for seamless connectivity in densely populated urban areas and broader rural coverage.

Compact in size at $24 \times 32 \times 1.6 \text{ mm}^3$, the suggested antenna has a minimum VSWR of 1.002, a maximum gain of 2.90 dB, and a maximum directivity of 4.13 dB for the operational frequency range. The slotted ground plane improves impedance matching and bandwidth. Additionally, the antenna achieves a highest efficiency of approximately 85.7%. With its simple structure and notable size reduction while maintaining strong performance, the mentioned antenna is a promising material for 5G systems. Although there are numerous works on patch antenna design in the literature related to 5G, most of the works are only simulation-based studies. However, in the present study, both the simulation and experimental work are conducted and the simulations are validated with the results of the experimental.

Table 2. The suggested antenna is compared to antennas that have already been designed

Ref. No.	Size (L × W × h) mm ³	Material of substrate/ ϵ_r	Frequency range (GHz)	f_c (GHz)	Loss of return (dB) at f_c	-10 dB BW (GHz)	Gain (dB)
[16]	150 × 80 × 0.8	FR-4/4.5	~1.27–1.5, ~2.2–2.5, ~3.5–4.2	~1.3, ~2.4, ~3.8	~-18, ~-18, ~-35	0.23, 0.3, 0.7	4.25
[29]	46 × 46 × 3.175	Rogers RT/2.2	2.44–2.54, 3.19–3.55	2.5, 3.2, 3.45	~-22	0.1, 0.36	-
[30]	35 × 35 × *	ECCOSTOCK HIK/10	3.30–4.38	3.9	~-38	1.08	5.96
[31]	40 × 28 × 1.6	FR-4/4.4	3.28–4.0	3.41, 3.83	-31.15	0.72	-
[32]	130 × 130 × *	FR-4/*	2.75–5.45	3.2, 4, 4.5	~-25	2.7	8.4
[33]	45 × 45 × 1.0	FR-4/4.4	1.82–2.92, 3.15–4.75	~2.4, ~3.7	~-40 ~-20	0.1, 1.6	4.8, 7.5
[34]	36 × 36 × 4	FR-4/4.4	2.8–3.81	3.47	-23	1.01	4.08
[35]	34 × 34 × 3.2	FR-4/4.3	~3.1–3.75	3.4	~-22	0.65	3.8
[36]	96 × 90 × *	Rogers RO4003C/3.38	3.24–3.8	~3.4, ~3.8	~-30	0.56	10.43
[37]	25 × 34.5 × 1.575	Rogers RT 5880/2.2	2.75–4.23	3.14	-34.24	1.48	2.77
This work	32 × 24 × 1.6	FR-4/4.3	2.6–5.8	3, 4.55	-58.5, -28.4	3.2	1.91 to 2.90

(*) not provided

3.10 Antenna fabrication and measurement

For validating the simulations, the structured antenna is fabricated, and the return loss is found in free space using LiteVNA 64 which has a measurement range of 50 Hz to 6.3 GHz. The glass fiber is used as the substrate during the fabrication due to the unavailability of pure FR-4 material. Figure 11 represent the structure of the fabricated antenna and Figure 12 illustrates the experimental setup for the measurement of the return loss of the manufactured antenna. The change in return loss (S11) with frequency acquired by the measurement with VNA and simulation is shown in Figure 13. As seen, the measured resonant peak positions are observed at 3.1 GHz and 3.9 GHz with the return loss of -56 dB and -29 dB, respectively. The graph also shows evidence of the wide bandwidth of the antenna.

The experimental results deviated from the simulated results because of the presence of some manufacturing defects such as pure FR-4 was not used as substrate, etc. The fluctuations or ripple in the measured data can be introduced by various means such material absorption, dispersion, scattering effect caused by the structural defects or quality of the materials used, connector loss and so on. Due to the unavailability of anechoic chamber, experimental results for radiation patten, gain and efficiency could not be obtained.

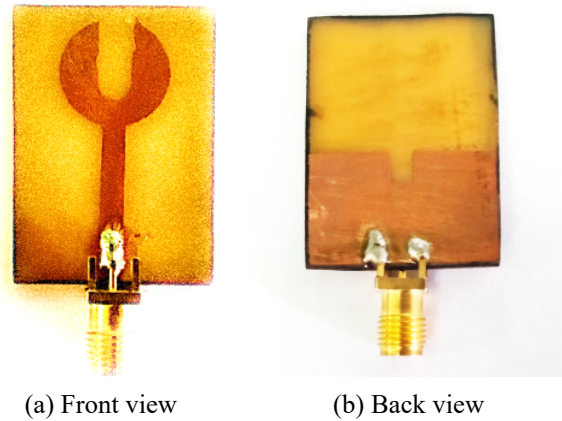


Figure 11. Fabricated prototype of the designed antenna

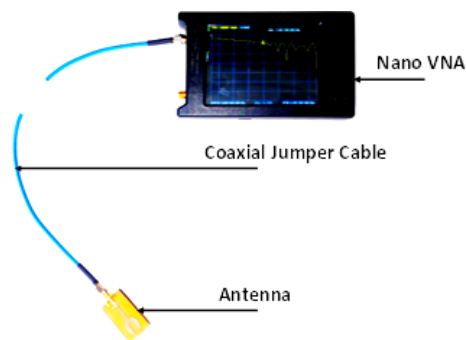


Figure 12. Experimental setup of the designed antenna

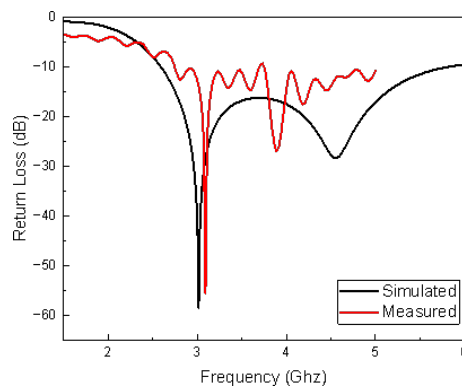


Figure 13. Measured and simulation results of return loss of the designed antenna

4. Conclusions

In this work, a new small open-ended wrench-shaped patch antenna with dimensions $24 \times 32 \times 1.6 \text{ mm}^3$ is designed and simulated using the CST Studio Suite to achieve Sub-6 GHz 5G band operation. The antenna is fed by a 50Ω micro-strip feed line and is etched on a FR-4 lossy dielectric substrate of height 1.6 mm, relative permittivity 4.3 and loss tangent 0.025. The simulation-based study shows adoption of slotted patch plane and defected ground structure enhances the bandwidth and impedance matching of antenna. The two resonant frequencies of proposed antenna are 3 GHz and 4.55

GHz, and the return losses are -58.5 dB and -28.4 dB, respectively. The antenna covers a broad 3.2 GHz impedance bandwidth with the frequency range of 2.6 to 5.8 GHz, which covers multiple key bands within the Sub-6GHz band used for different 5G applications. A maximum gain of 2.90 dB, directivity of 4.13 dBi, and radiation efficiency of 85.7% are attained in this frequency region. Significant downsizing is achieved while preserving the necessitate performance characteristics suitable for Sub-6GHz 5G wireless communication devices. The developed antenna is constructed as an experimental prototype, and the measured return loss findings show quite well alignment with the simulated results.

Conflict of interest

The authors declare no conflict of interest.

References

- [1] L. C. Paul, S. S. A. Ankan, T. Rani, M. Karaaslan, M. N. Hossain, A. J. A. Al-Gburi, et al., "A wideband highly efficient omnidirectional compact antenna for WiMAX/lower 5G communications," *Int. J. RF Microw. Comput. Aided Eng.*, vol. 2023, p. 7237444, 2023. <https://doi.org/10.1155/2023/7237444>
- [2] M. Shakir, S. Aslam, M. U. Sarwar, M. Adnan, and M. R. Khan, "Performance evaluation and design of 5G communication-based millimeter wave antenna," *EURASIP J. Wireless Commun. Netw.*, vol. 2021, no. 1, pp. 1–10, 2021. <https://doi.org/10.1186/s13638-021-02052-9>
- [3] L. C. Paul, A. K. Sarkar, M. A. Haque, P. Miah, P. M. Ghosh, and M. R. Islam, "Investigation of the dependency of an inset feed rectangular patch antenna parameters with the variation of notch width for WiMAX applications," in *Proc. IEEE Int. Conf. Electron., Commun. Aerosp. Technol. (ICECA)*, Coimbatore, India, Mar. 29–31, 2018, pp. 151–154. <https://doi.org/10.1109/ICECA.2018.8474908>
- [4] R. Y. Kumar, S. Kamatham, and S. Peddakrishna, "CPW-fed penta band monopole antenna for multiservice wireless applications," *Adv. Technol. Innov.*, vol. 7, no. 1, pp. 66–76, Jan. 2022. <https://doi.org/10.46604/aiti.2021.8434>
- [5] M. W. Tian, L. Wang, S. R. Yan, X. X. Tian, Z. Q. Liu, and J. J. P. C. Rodrigues, "Research on financial technology innovation and application based on 5G network," *IEEE Access*, vol. 7, pp. 138614–138623, 2019. <https://doi.org/10.1109/ACCESS.2019.2936860>
- [6] D. Imran, M. M. Farooqi, M. I. Khattak, Z. Ullah, M. I. Khan, M. A. Khattak, et al., "Millimeter wave microstrip patch antenna for 5G mobile communication," in *Proc. Int. Conf. Eng. Emerg. Technol. (ICEET)*, Lahore, Pakistan, Feb. 22–23, 2018, pp. 1–6. <https://doi.org/10.1109/ICEET1.2018.8338623>
- [7] L. C. Paul, M. T. R. Jim, T. Rani, S. S. A. Ankan, S. C. Das, and H. K. Saha, "A pi-shaped slotted patch antenna with a partial ground structure for lower 5G/WiFi/WiMAX applications," *Heliyon*, vol. 8, no. 10, p. e10934, Oct. 2022. <https://doi.org/10.1016/j.heliyon.2022.e10934>
- [8] A. H. Abdelgwad, "Microstrip patch antenna enhancement techniques," *Int. J. Electron. Commun. Eng.*, vol. 12, no. 10, pp. 703–710, 2018. <http://scholar.waset.org/1307-6892/10009601>
- [9] L. C. Paul, H. K. Saha, T. Rani, M. Z. Mahmud, T. K. Roy, and W. S. Lee, "An omni-directional wideband patch antenna with parasitic elements for Sub-6 GHz band applications," *Int. J. Antennas Propag.*, vol. 2022, p. 9645280, 2022. <https://doi.org/10.1155/2022/9645280>
- [10] I. Ishteyaq, L. S. Masoodi, and K. Muzaffar, "A compact double-band planar printed slot antenna for sub-6GHz 5G wireless applications," *Int. J. Microw. Wireless Technol.*, vol. 13, no. 5, pp. 469–477, 2021. <https://doi.org/10.1017/S1759078720001269>
- [11] S. K. Goudos, A. Tsiflikiotis, D. Babas, K. Siakavara, C. Kalialakis, and G. K. Karagiannidis, "Evolutionary design of a dual band E-shaped patch antenna for 5G mobile communications," in *Proc. 6th Int. Conf. Mod. Circ. Syst. Technol. (MOCAS)*, Thessaloniki, Greece, May 4–6, 2017, pp. 1–4. <https://doi.org/10.1109/MOCAS.2017.7937640>
- [12] C. Zebiri, D. Sayad, I. Elfergani, A. Iqbal, W. F. Mshwat, J. Kosha, et al., "A compact semi-circular and arc-shaped slot antenna for heterogeneous RF front-ends," *Electronics*, vol. 8, no. 10, p. 1123, Oct. 2019. <https://doi.org/10.3390/electronics8101123>

- [13] F. F. Hashim, W. N. L. B. W. Mahadi, T. B. A. Latef, and M. B. Othman, "Fabric-metal barrier for low specific absorption rate and wide-band felt substrate antenna for medical and 5G applications," *Electronics*, vol. 12, no. 12, p. 2754, Jun. 2023. <https://doi.org/10.3390/electronics12122754>
- [14] M. E. Yassin, H. A. Mohamed, E. A. Abdallah, and H. S. El-Hennawy, "Single-fed 4G/5G multiband 2.4/5.5/28 GHz antenna," *IET Microw. Antennas Propag.*, vol. 13, no. 3, pp. 286–290, 2019. <https://doi.org/10.1049/iet-map.2018.5122>
- [15] B. G. Hakanoglu, O. Sen, and M. Turkmen, "A square microstrip patch antenna with enhanced return loss through defected ground plane for 5G wireless networks," in *Proc. 2nd URSI Atlantic Radio Sci. Meeting (AT-RASC)*, Gran Canaria, Spain, May 28–Jun. 1, 2018, pp. 1–4. <https://doi.org/10.23919/URSI-AT-RASC.2018.8471618>
- [16] M. Khalifa, L. Khashan, H. Badawy, and F. Ibrahim, "Broadband printed-dipole antenna for 4G/5G smartphones," *J. Phys.: Conf. Ser.*, vol. 1447, no. 1, p. 012049, 2020. <https://doi.org/10.1088/1742-6596/1447/1/012049>
- [17] A. Kapoor, R. Mishra, and P. Kumar, "Wideband miniaturized patch radiator for Sub-6GHz 5G devices," *Heliyon*, vol. 7, no. 9, p. e07931, Sep. 2021. <https://doi.org/10.1016/j.heliyon.2021.e07931>
- [18] H. Santos, P. Pinho, and H. Salgado, "Patch antenna-in-package for 5G communications with dual polarization and high isolation," *Electronics*, vol. 9, no. 8, p. 1223, Aug. 2020. <https://doi.org/10.3390/electronics9081223>
- [19] A. Z. M. Imran, M. L. Hakim, M. Ahmed, M. T. Islam, and E. Hossain, "Design of microstrip patch antenna to deploy unmanned aerial vehicle as UE in 5G wireless network," *Int. J. Electr. Comput. Eng.*, vol. 11, no. 5, pp. 4202–4213, Oct. 2021. <https://doi.org/10.11591/ijece.v11i5.pp4202-4213>
- [20] M. Rahman and J. D. Park, "The smallest form factor UWB antenna with quintuple rejection bands for IoT applications utilizing RSR and RCSRR," *Sensors*, vol. 18, no. 3, p. 911, Mar. 2018. <https://doi.org/10.3390/s18030911>
- [21] M. J. Jeong, N. Hussain, H. U. Bong, J. W. Park, K. S. Shin, S. W. Lee, et al., "Ultrawideband microstrip patch antenna with quadruple band notch characteristic using negative permittivity unit cells," *Microw. Opt. Technol. Lett.*, vol. 62, no. 2, pp. 816–824, 2020. <https://doi.org/10.1002/mop.32078>
- [22] R. Azim, R. Aktar, A. K. M. M. H. Siddique, L. C. Paul, and M. T. Islam, "Circular patch planar ultra-wideband antenna for 5G sub-6GHz wireless communication applications," *J. Optoelectron. Adv. Mater.*, vol. 23, pp. 127–133, 2021.
- [23] L. C. Paul, S. C. Das, N. Sarker, R. Azim, M. F. Ishraque, and S. A. Shezan, "A wideband microstrip patch antenna with slotted ground plane for 5G application," in *Proc. Int. Conf. Sci. Contemp. Technol.*, Dhaka, Bangladesh, Aug. 5–7, 2021, pp. 1–5. <https://doi.org/10.1109/ICSCT53883.2021.9642597>
- [24] L. C. Paul, H. K. Saha, T. K. Roy, R. Azim, and M. T. Islam, "A wideband inset-fed simple patch antenna for sub-6GHz band applications," in *Proc. Int. Conf. Innov. Sci. Eng. Technol.*, Chittagong, Bangladesh, Feb. 26–27, 2022, pp. 106–110. <https://doi.org/10.1109/ICISSET54810.2022.9775926>
- [25] M. S. Ellis, Z. Zhao, J. Wu, Z. Nie, and Q. H. Liu, "Unidirectional planar monopole ultra-wideband antenna using wrench-shaped feeding structure," *Electron. Lett.*, vol. 50, no. 9, pp. 654–655, 2014. <https://doi.org/10.1049/el.2014.0298>
- [26] R. N. Tiwari, P. Singh, B. K. Kanaujia, and A. K. Pandit, "A coalesced kite shaped monopole antenna for UWB technology," *Wireless Personal Commun.*, vol. 114, pp. 3031–3048, 2020. <https://doi.org/10.1007/s11277-020-07516-7>
- [27] R. N. Tiwari, P. Singh, and B. K. Kanaujia, "A modified microstrip line fed compact UWB antenna for WiMAX/ISM/WLAN and wireless communications," *AEU-Int. J. Electron. Commun.*, vol. 104, pp. 58–65, 2019. <https://doi.org/10.1016/j.aeue.2019.03.008>
- [28] K. P. Ray, M. D. Pandey, and S. Krishnan, "Determination of resonance frequency of hexagonal and half hexagonal microstrip antennas," *Microw. Opt. Technol. Lett.*, vol. 49, no. 11, pp. 2876–2879, 2007. <https://doi.org/10.1002/mop.22843>
- [29] S. Nelaturi, "ENGTL based antenna for Wi-Fi and 5G," *Analog Integr. Circ.*, vol. 107, no. 1, pp. 165–170, 2021. <https://doi.org/10.1007/s10470-020-01766-y>
- [30] J. Iqbal, U. Illahi, M. N. M. Yasin, M. A. Albreem, and M. F. Akbar, "Bandwidth enhancement by using parasitic patch on dielectric resonator antenna for sub-6GHz 5G NR bands application," *Alexandria Eng. J.*, vol. 61, no. 6, pp. 5021–5032, 2022. <https://doi.org/10.1016/j.aej.2021.09.049>
- [31] A. Kapoor, R. Mishra, and P. Kumar, "Compact wideband-printed antenna for sub-6GHz fifth-generation applications," *Int. J. Smart Sens. Intell. Syst.*, vol. 13, no. 1, pp. 1–10, 2020. <https://doi.org/10.21307/ijssis-2020-033>
- [32] B. Huang, W. Lin, J. Huang, J. Zhang, G. Zhang, and F. Wu, "A patch/dipole hybrid-mode antenna for sub-6GHz communication," *Sensors*, vol. 19, no. 6, p. 1358, 2019. <https://doi.org/10.3390/s19061358>
- [33] Z. Yu, L. Huang, Q. Gao, and B. He, "A compact dual-band wideband circularly polarized microstrip antenna for sub-6G application," *Prog. Electromagnet. Res. Lett.*, vol. 100, pp. 99–107, 2021. <https://doi.org/10.2528/PIERL21082702>

- [34] R. Swetha and L. Anjaneyulu, "Novel design and characterization of wide band hook shaped aperture coupled circularly polarized antenna for 5G application," *Prog. Electromagnet. Res. C*, vol. 113, pp. 161–175, 2021. <https://doi.org/10.2528/PIERC21040202>
- [35] Y. I. Al-Yasir, A. S. Abdullah, N. O. Parchin, R. A. Abd-Alhameed, and J. M. Noras, "A new polarization-reconfigurable antenna for 5G applications," *Electronics*, vol. 7, no. 11, p. 293, 2018. <https://doi.org/10.3390/electronics7110293>
- [36] J. Park, M. Jeong, N. Hussain, S. Rhee, S. Park, and N. Kim, "A low-profile high-gain filtering antenna for fifth generation systems based on nonuniform metasurface," *Microw. Opt. Technol. Lett.*, vol. 61, no. 11, pp. 2513–2519, 2019. <https://doi.org/10.1002/mop.31931>
- [37] L. C. Paul, S. A. Hye, T. Rani, M. I. Hossain, M. Karaaslan, P. Ghosh, et al., "A compact wrench-shaped patch antenna with a slotted parasitic element and semi-circular ground plane for 5G communication," *e-Prime Adv. Elec. Eng. Electron. Energy*, vol. 6, p. 100334, Dec. 2023. <https://doi.org/10.1016/j.prime.2023.100334>